Experimental investigation of excitonic spin relaxation dynamics in GaN

Christelle Brimont, Mathieu Gallart, Olivier Crégut, Bernd Hönerlage, and Pierre Gilliot
IPCMS—GONLO Unité mixte CNRS—ULP (UMR 7504), 23 rue du Læss, Boîte Postale 43, 67034 Strasbourg Cedex 2, France
(Received 3 October 2007; revised manuscript received 24 January 2008; published 3 March 2008)

By performing nondegenerate pump-probe experiments, we study the relaxation dynamics of spin-polarized A and B excitons in wurtzite epitaxial GaN. By analyzing the differential reflectivity spectra ($\Delta R/R$) of the two circularly polarized probe components, we are able to identify each spin relaxation channel (electron, light- and heavy-hole spin flips) separately and to extract characteristic times of the different spin relaxation processes. In addition, spectral oscillatory features are observed for negative delays. They show a rapid rise determined by the fast dephasing time T_2 of the excitonic transitions. We show that the high density of dislocations increases the spin relaxation of electrons and holes through the Elliot–Yafet mechanism and makes the exciton dephasing time very short. The measured heavy-hole relaxation time, which is not extremely short compared to the electron relaxation time, can be related to the band structure, in which the degeneracy between different spin valence bands is partially lifted.

DOI: 10.1103/PhysRevB.77.125201 PACS number(s): 78.47.−p, 72.25.Fe, 72.25.Rb, 73.61.Ey

INTRODUCTION

Gallium nitride (GaN) and its related alloys have been extensively studied in the past ten years for their light emitting properties (see, for example, Ref. 1 and references therein) and are now intensively used in optoelectronic devices emitting in the blue and UV region of the optical spectrum. Because of their wide band gap (~3.5 eV for GaN), nitride based nanostructures show carrier-confinement energies of several hundreds of meV. Quantum dots are, for example, expected to operate at room temperature and are promising for applications, such as single-photon sources or in spintronics. However, few experimental data can be found in the literature concerning the experimental investigation of spin physics in nitride compounds.[2] Spin relaxation in bulk GaN was investigated by time-resolved spin-dependent pump and probe reflectance measurements[3–5] or by using spectrally resolved four-wave mixing techniques.[6] Nevertheless, the signals from the different excitons were not distinguished in these experiments. Here, we present measurements of the exciton-spin dynamics using nondegenerate spectrally and temporally resolved pump-probe experiments: Circularly polarized pump pulses excite resonantly a population of A excitons in a thick GaN layer. We then measure simultaneously the differential reflectivity ($\Delta R/R$) spectra of the two circular components of a broadband probe, which is linearly polarized, as a function of the delay between pump and probe pulses.

SAMPLE AND EXPERIMENTAL SETUP

The sample we study is a 3 μm thick wurtzite GaN epilayer grown by metallo-organic chemical vapor deposition[7] on a *c* plane of sapphire. Its typical residual *n* type doping results in a density of about 5×10^{16} cm^{-3}. Its **c** axis is perpendicular to the substrate. In wurtzite GaN, the crystalline field and the spin-orbit interaction lift the valence band degeneracy at the Γ point of the Brillouin zone. From the three valence subbands, with Γ_9, Γ_7, and Γ_7 symmetry, and the Γ_7 conduction band, one can build three exciton series labeled A, B, and C.[8] Linear reflectance and photoluminescence spectra from our sample are displayed in Fig. 1: Energy splittings are 8 meV between A and B, and 19 meV between A and C excitons. Thus, in our experiments performed at low temperatures, we can neglect C-exciton populations since they will not be created by the pump pulses nor thermally excited. We will, therefore, focus in this work on the A and B excitons. Their electrons have a $s_z=\pm1/2$ spin and they involve, respectively, heavy holes with pseudospin $j_z=\pm3/2$ and light holes with $j_z=\pm1/2$ (see inset of Fig. 4). The resulting exciton pseudospin states $|\pm1\rangle_A$, $|\pm1\rangle_B$ are optically active, while both $|\pm2\rangle_A$ and $|0\rangle_B$ states are dark states when exciting with the electric field polarization perpendicular to **c**.

The pump-probe experimental setup that we use is shown in Fig. 2. The laser source is a homemade titanium: sapphire oscillator. It generates 80 fs pulses at 82 MHz which pass a regenerative amplifier, working at 200 kHz, before being sent into two optical parametric amplifiers (OPAs) which generate, respectively, pump and probe pulses.

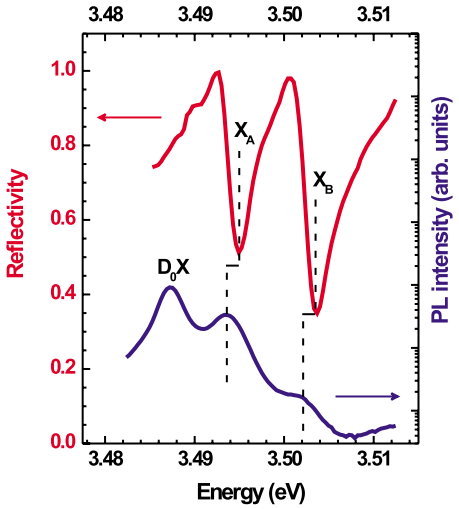

FIG. 1. (Color online) Low temperature linear reflectivity and photoluminescence spectra.

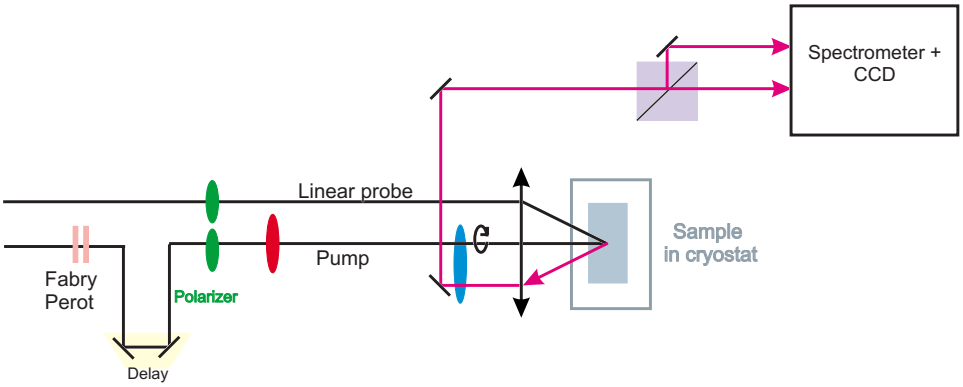

FIG. 2. (Color online) Optical setup of the temporally and spectrally resolved pump-probe experiment.

Both OPAs are tuned close to 710 nm (1.746 eV). Pulses are further compressed and spectrally filtered by optical compressors using a pair of prisms and a spatial filter. Their duration is then close to 50 fs. With two BBO crystals, the pulses are frequency-doubled to reach the GaN exciton spectral region (about 3.492 eV). The doubling process increases the pulse duration to an estimated value of ~200 fs.

The pump pulses are spectrally filtered through a Fabry–Pérot cavity to a spectral width of $\Delta E = 5.46$ meV full width at half maximum (FWHM). The Fabry–Pérot transmittance is described by the Airy function, which is a periodic succession of peaks whose spectral profile is quasi-Lorentzian. This corresponds, in the time domain, to the sum of the multiple pulse reflections. It gives rise to an asymmetric temporal profile with a rise time that remains the same as the unfiltered one (~100 fs), whereas the decay time exhibits an exponential decay with a characteristic time constant that can be as short as $\tau = 2\hbar\Delta E^{-1} \sim 250$ fs. Pulses are circularly polarized and, thus, selectively excite the A-excitonic transition with total angular momentum $|+1\rangle_A$. The energy per pulse is 10 nJ, that is to say, after focusing onto the sample $\sim 1.8 \times 10^{14}$ cm^{-2} photons at an energy of 3.5 eV. The Fabry–Pérot cavity is tuned by minimizing the photoluminescence of the B exciton.

The broadband linearly polarized probe pulses extend spectrally over both A- and B-excitonic transitions. A quarter-wave plate transforms the two circularly polarized components of the probe beam, reflected in normal incidence, into two linearly polarized, mutually perpendicular components, which are separated by a linear polarizer cube. The two beams are then directed at different heights onto the entrance slit of a spectrometer and are detected as two-different spectra on our two dimensional charge coupled device camera. In this way, the two circular components of the reflected probe pulses are registered simultaneously as a function of the pump-probe delay time. For each time delay, the two reflected probe spectra are recorded in the presence and then in the absence of the pump pulse excitation and two $\Delta R/R$ spectra are calculated, one for each probe polarization (σ^- and σ^+). In all measurements, the sample temperature is kept at 9 K in a cold-finger cryostat.

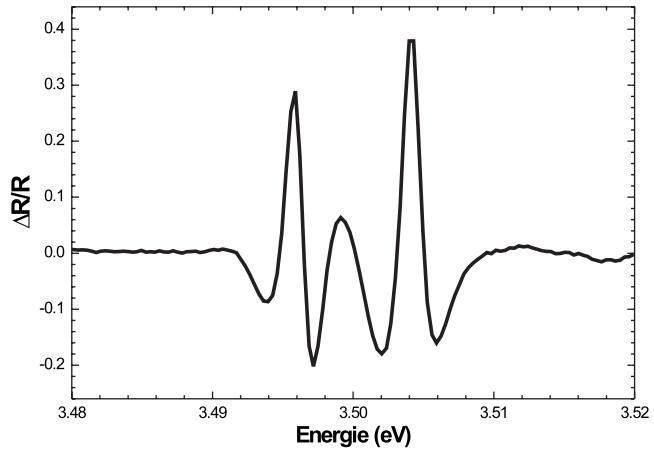

FIG. 3. $\Delta R/R$ for a negative delay of −0.1 ps (pump after probe pulses).

EXPERIMENTAL RESULTS AND DISCUSSION

Typical differential reflectivity ($\Delta R/R$) spectra are shown in Figs. 3 and 4. For negative time delays (Fig. 3), i.e., when the probe pulse arrives before the pump pulse, $\Delta R/R$ displays spectral oscillatory features in the vicinity of the excitonic resonances. This phenomenon is due to the sudden perturbation by the pump pulse of the polarization induced by the probe pulse:[9] When the probe pulse is sent to the sample,

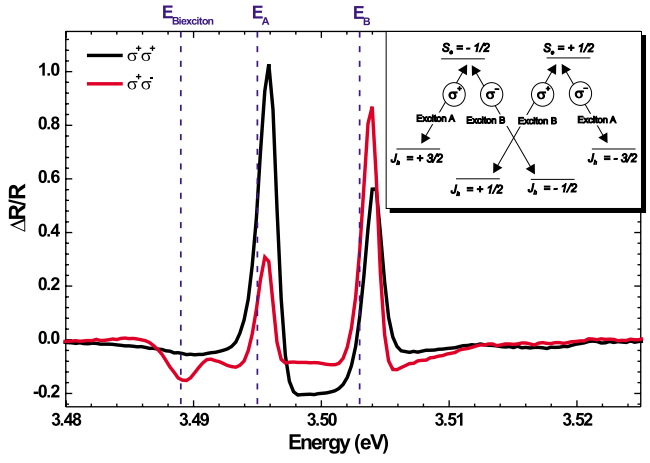

FIG. 4. (Color online) $\Delta R/R$ spectra for co- and counterpolarized configurations of the pump and probe pulses and a delay of 1 ps. The inset shows the optical selection rules for GaN at the Γ point of the first Brillouin zone.

it generates a first order polarization, decaying with the dephasing time T_2. The third order polarization, which is emitted in the probe direction when the delayed pump pulse impinges, interferes with the polarization left from the probe pulse. We can consider, for example, a very short pump pulse, which can be approximated by a delta function and which induces an oscillator strength variation of a single resonance. The perturbation induced in the medium shows then a steplike function temporal profile and the $\Delta R/R$ spectral shape yields:[9]

$$\frac{\Delta R}{R}(\omega) \propto \frac{\exp(\tau_{TP}/T_2)}{T_2} \frac{T_2(\omega-\omega_0)\sin\,\tau_{TP}(\omega-\omega_0)+\cos\,\tau_{TP}(\omega-\omega_0)}{(\omega-\omega_0)^2+(1/T_2)^2}$$

where τ_{TP} is the delay between probe and pump pulses ($\tau_{\mathrm{TP}}<0$) and ω_0 is the resonance pulsation. The coherent spectral oscillations have a period inversely proportional to the time delay between the pump and probe pulses. Moreover, the rise time of the $\Delta R/R$ signal is given by the dephasing time T_2.

Let us now discuss the case of a pump pulse with a finite duration. The oscillatory features in the above expression originate mainly from the discontinuity of the temporal response induced by the pump pulse: its abrupt variation in the time domain brings about oscillations in the spectral domain. In other words, to observe the oscillations, the rise time of the pump pulse must be sufficiently small with respect to T_2. This condition is fulfilled in our experiment and we can, thus, extract the polarization dephasing time by an exponential fit of the $\Delta R/R$ signal rise time. We find $T_2=0.3$ ps for both A and B excitons. These values are comparable to those previously obtained by four-wave mixing experiments,[10–15] where T_2 values lie in a range from a few hundred femtoseconds to a few picoseconds. Moreover, our T_2 value is equivalent to a 4 meV homogeneous broadening, which is in agreement with the excitonic linedwidth observed in our photoluminescence experiments (see Fig. 1). This coherence time that we measure is very short, showing that excitons encounter collision processes which are very efficient in dephasing them. This can be related to a large number of dislocations in the crystalline layer. These typical structural defaults of nitride compounds are due to the heteroepitaxy of GaN on the lattice unmatched sapphire substrate.[24] We can, thus, suppose that exciton collisions with these defaults are responsible for the very fast decrease of their optical coherence. This assumption about the imperfection density is in good agreement with the spin relaxation that we identify in the following and which will be shown to be dominated by the dislocation assisted Elliot–Yafet (EY) mechanism.

The $\Delta R/R$ spectra at a positive time delay of 1 ps are shown in Fig. 4 for the two different probe helicities. They exhibit two resonances, related to the A and B excitons. Their amplitudes are different and depend on the probe polarization, as expected from the optical selection rules shown in the inset of Fig. 4. This indicates that a spin-polarized population of excitons is actually photocreated. Because A and B excitons share the same conduction band, a population of $|+1\rangle_{\mathrm{A}}$ excitons modifies also the oscillator strength of the $|-1\rangle_{\mathrm{B}}$ excitons. A $\Delta R/R$ signal is, therefore, expected at the B exciton energy, but only for a σ^- polarized probe. However, a $\Delta R/R$ signal is also observed at the B exciton energy at zero delay for the σ^+ probe polarization despite the use of a spectrally filtered pump pulse. We have carefully checked that the ΔR signal is linear in pump intensity. Hence, decreasing the pump intensity only affects the signal to noise ratio, with the spectral shape remaining the same. In particular, the instantaneous signal at the B-exciton energy in cocircular configuration is still present. We, thus, attribute the signal at the $|+1\rangle_{\mathrm{B}}$ to the $\mathbf{k}\cdot\mathbf{p}$ mixing at finite wave vectors between the three subvalence bands. In particular, for light propagating along the c axis, the valence band Hamiltonian exhibits a coupling term between heavy-hole (HH) and light-hole (LH) bands, which is proportional to the squared in-plane wave vector $k_{\pm}=k_x \pm ik_y$.[16] Indeed, the excitonic Bohr radius a_B in GaN is close to 3 nm. The wave function of the exciton develops in k space up to $a_B^{-1}=0.03$ Å^{-1}. For this value of $\mathbf{k}$, we have calculated that the hole envelope function is roughly 70% HH and 30% LH. So, although no $|+1\rangle_{\mathrm{B}}$ excitons are pump created in the sample, the phase space filling of the LH bands is responsible for the $\Delta R/R$ signal at B-exciton energy for σ^+ polarized probe.

In the particular case of a σ^- probe, an induced reflection signal can be seen 6 meV below the A-excitonic resonance. Figure 1 displays linear reflectivity and photoluminescence spectra at low temperature. As usually seen in bulk semiconductors, the photoluminescence spectrum is dominated by the donor bound exciton whose energy lies ~6 meV below the A exciton: compared to free A and B excitons, the donor localized state constitutes a very efficient recombination center, preventing the exciton from nonradiative escape. However, no structure emerges in the linear reflectivity spectrum. This means that no significant density of electronic states, which is the physical quantity probed by linear reflectivity and pump-probe experiment, is related to the impurities. It is, thus, not possible that the induced signal which is observed in our sample would be due to bound excitons. We interpret this feature as an induced exciton-biexciton transition, with 6 meV being close to previously reported biexciton binding energy.[17] Moreover, the signal is proportional to the exciton density and does not emerge in the linear spectrum. This induced transition disappears as fast as the $|+1\rangle_{\mathrm{A}}$ excitonic population relaxes. In agreement with the selection rules, this signal is not present in the case of a σ^+ σ^+ polarization sequence. Furthermore, no increase of the σ^+ σ^- $\Delta R/R$ signal

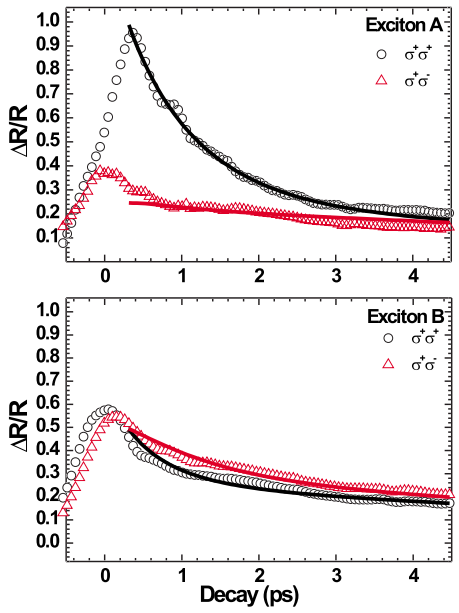

FIG. 5. (Color online) Spectrally integrated $\Delta R/R$ decays for co- and counterpolarized configurations of the pump and probe pulses.

on the A exciton is observed when the σ^+ σ^+ $\Delta R/R$ decreases. These facts evidence that the loss of the $|+1\rangle_A$ excitonic population does not feed directly the $|-1\rangle_A$ pseudospin state, as it would be in the case of a simultaneous spin flip of electron and hole. In other words, relaxation of the exciton as a whole, where the joint electron and hole spin flips populate the $|-1\rangle_A$ state, presents a negligible contribution with respect to the spin relaxations of the individual carriers, which first populate the dark $|\pm 2\rangle_A$ exciton states. Only subsequent electron and hole spin flips allow a $|-1\rangle_A$ state population to build up from the initial $|+1\rangle_A$ one.

The spectrally integrated $\Delta R/R$ decays for the four bright excitons are displayed in Fig. 5. The duration of the nonlinear $\Delta R/R$ signal is limited by the relaxation of the different spin populations: by making progressively equal the $|+1\rangle$ and $|-1\rangle$ excitonic populations, the relaxation of the excitonic spins leads to the equalization of the $\Delta R/R$ signals for the two polarization configurations. We analyze the experimental data using the method explained in Ref. 33. The exciton wave functions develop on electron and hole states: From the two hole A bands with spins $j=3/2$, $j_z=\pm 3/2$ and the two hole B bands with spins $j=3/2$, $j_z=\pm 1/2$, combined with the electron band with spins $s=1/2$, $s_z=\pm 1/2$, eight excitonic states $|\pm 1\rangle_A$, $|\pm 1\rangle_B$, $|\pm 2\rangle_A$, $|0\rangle_B$ are built. The phase space filling of the valence and conduction bands is, thus, responsible for the modification of the excitonic oscillator strengths that we measure in the $\Delta R/R$ signal. One should note that an induced signal can be observed on an exciton transition, even if there is no exciton population, because it shares a common band and spin with the excitons, which are created by the pump or which result from relaxation processes. These populations of the $|\pm 1\rangle_A$, $|\pm 1\rangle_B$ $|\pm 2\rangle_A$, $|0\rangle_B$ states and their time evolution are modeled using a dynamic multilevel model[32,35] that contains rate equations involving the different spin relaxation processes and excitonic recombination. From the corresponding filling of the bands and spin states, the corresponding differential reflections for each excitonic transition are then deduced and compared to the measured $\Delta R/R$ signals. This allows us to extract, for each spin relaxation channel (electron, light- and heavy-hole spin flips), the characteristic time constants. The best fit, according to our model, is plotted in Fig. 5. We determine the spin relaxation time of the electron in the conduction band $T_e=15$ ps, the spin relaxation time of the heavy hole $T_{HH}=5$ ps, and the spin relaxation time of the light hole $T_{LH}=1.5$ ps. The accuracy of these numerical values is limited by the short lifetimes of the A- and B-excitonic populations, which are $T_A=1.5$ ps and $T_B=3.4$ ps, respectively. We attribute these short decays to the relaxation of free excitons toward localization centers, like donors whose photoluminescence is seen to be very intense in our sample. It is important to note that all spin relaxation times given above are necessary to correctly fit the dynamics of the observed signals.

The spin polarization of the photocreated excitons persists on a time scale of some picoseconds. This is comparable to values given in previous works published on undoped wurtzite GaN.[3,4,6] However, the comparison remains difficult because, in previous works, the spin relaxation rates for each kind of carriers are not resolved. In Ref. 6, the authors performed a spin grating experiment on a 70 μm thick metallo-organic vapor phase epitaxy grown wurtzite GaN layer. They used 200 fs pulses with 13 meV FWHM. As stated by the authors, it was then impossible to achieve the selective excitation of individual exciton levels. The authors interpret the spin relaxation in terms of the Bir–Aronov–Pikus (BAP) mechanism,[18] which involves the relaxation of the excitonic spin as a whole, because of the strong exchange interaction in GaN. At this point, our conclusion is different: because, in our case, an induced ΔR signal toward biexciton state does not show up in the σ^+ σ^+ configuration, we conclude that the $|-1\rangle$ excitonic state is not significantly populated. Thus, the BAP mechanism cannot be the main process of the spin relaxation in our case. Otake *et al.*[4] measured the spin relaxation of acceptor-bound exciton in a 2.2 μm thick wurtzite GaN layer and also explained it through the BAP process. In that case, it is reasonable to think that the localization of the exciton prevents it from scattering and from spin relaxation: as the electron and hole wave functions overlap, the BAP process, which is due to the e-h exchange interaction, is enhanced compared to the other mechanisms involving the spin relaxation of individual carriers.

The experimental conditions in the work by Kuroda *et al.*[3] are very close to ours: they performed pump and probe reflectivity measurements on a 2.2 μm GaN epilayer to determine the spin relaxation rate of free A excitons. The authors tuned the pump wavelength in order to populate only the A-exciton level. The spin polarization reaches 60% at zero delay between pump and probe, a value which is similar to our result. However, we have discussed above that the valence band mixing at finite wave vectors results in a contribution to the ΔR signal at the B-exciton energy even if the excitation is tuned to the A-exciton resonance. Our work gives supplementary information because the ΔR signal is spectrally resolved: we are able to discriminate the role of the different excitons and, so also, to extract quantitative data

for the different spin relaxation channels. Our results enlighten the fact that, for free excitons, the spin relaxation of each carrier taken separately is more efficient than the relaxation of the total excitonic spin. This conclusion is in agreement with Ref. 3, where the defect assisted EY[19,20] process is invoked to explain the spin relaxation. This assumption is supported by the temperature dependence of the relaxation rate.[3]

This interpretation is interesting because the EY relaxation rate is proportional to the scattering rate, which is expected to be large in an imperfect material such as wurtzite GaN layers. Then it would be useful to compare our numerical results and those from literature to a theoretical estimation of the spin relaxation times. Unfortunately, existing theoretical works deal with spin physics in zinc-blende GaN and with a comparison with GaAs. In particular, Yu et *et al.*[21] calculated the spin relaxation rate for electrons and heavy and light holes in cubic GaN, taking into account the EY and D'yakonov–Perel[22] mechanisms. They include scattering from ionized dopants, whose concentration is taken equal to 10^{16} cm^{-3}, and longitudinal optical phonons. They found that heavy- and light-hole relaxation times are in the range of 10^{-2} ps and that electron relaxation time can reach 10^{4} ps. Jena[23] calculated the spin relaxation time of electrons in zinc-blende GaN, taking into account scattering on edge dislocations. The core of a dislocation is charged and its Coulombic potential leads to the scattering of electrons in the conduction band.

Threading dislocations are the main structural defects in GaN and are known to be responsible for nonradiative recombination of excitons (see, for example, Ref. 24). For a given sample temperature, the spin relaxation time of the dislocation assisted EY process is linear with the dislocation density N_d. At low temperature, for $N_d=10^8$, $T_e \sim 1$ ns. The theoretical works of Refs. 21 and 23 seem to be confirmed by the result obtained by Takeuchi *et al.*,[5] who extracted a spin lifetime on the nanosecond scale in zinc-blende GaN. In their work, the spin relaxation is not resolved into electron and hole spin relaxations. Nevertheless, we can argue that the degeneracy of the valence bands at the gamma point is probably responsible for a fast relaxation of the hole spin in the zinc-blende structure and that the long lasting signal is due to the electron spin.

Considering this, we can give some hypothesis concerning the spin relaxation mechanism in our sample. The first process for the spin relaxation is the dislocation assisted EY mechanism. Indeed, from the calculation of Ref. 23, the spin relaxation time constant of the electron in zinc-blende GaN lies in the range of 1–0.01 ns for a dislocation density varying from 10^8 to 10^{10} cm^{-3}, which are typical dislocation densities in wurtzite GaN.[24] These time constants are consistent with our value of $T_e=15$ ps.

Concerning the holes, the time constants we have determined are not extremely short with regard to the electron spin relaxation time as in the bulk material [as, e.g., GaAs (Ref. 25)] and are slightly longer than what is expected theoretically in zinc-blende GaN.[21] This can be explained if one takes into account the structure of the valence band in wurtzite GaN. Indeed, in bulk semiconductors with zinc-blende structure, the HH and LH bands are degenerated at the Γ point and the spin of the photocreated holes relaxes quickly (typically in a few hundreds of femtoseconds[26]). Lifting the degeneracy at the Γ point slows down the spin relaxation. This effect was predicted by theory[27,28] and observed by many authors studying spin relaxation in GaAs/AlGaAs quantum wells,[29–35] where stresses split light- and heavy-hole bands. In this particular case, previous works have shown[25] that $T_{\mathrm{HH}} \sim (\Delta E_{\mathrm{HH-LH}})^x$, with $x=3.2$, and can reach a few tenths of picoseconds for $\Delta E_{\mathrm{HH-LH}} \sim 10$ meV. In our GaN sample, the crystal field plays the same role as the confinement effect by lifting the valence band degeneracy, and the splitting between the light and heavy holes is 8 meV, which is comparable with the situation seen in the GaAs quantum wells.

In semiconductors, the relaxation of the hole pseudospin is influenced by the admixture of the valence subbands. The LH band, because of the small value of the spin-orbit interaction in GaN ($\sim$15 meV), remains strongly coupled with the split off (SO) band for zero wave vector. Thus, the B exciton is built from a combination of the LH and SO subbands, which favors a faster spin dynamics: $T_{\mathrm{LH}}=1$ ps.

CONCLUSION

We have measured the spin dynamics of spin polarized excitons in epitaxial GaN using a nondegenerate spectrally resolved pump-probe differential reflectivity experiment. The coherent spectral oscillations observed for negative time delays allow us to determine the exciton dephasing time, which is quite short ($T_2=0.3$ ps) because of exciton collisions with dislocations. We demonstrate from the observation of an exciton-biexciton induced transition that the spin flip of the exciton as a whole is negligible with regard to the spin relaxation of the individual carriers. By fitting the $\Delta R/R$ decay for positive time delays at the A and B resonances, using a multilevel model which takes into account both bright and dark exciton states, we extract the spin relaxation times of electrons and holes. We show that the EY mechanism is dominant because of the density of dislocations and that the quite long HH relaxation time can be related to the band structure of wurtzite gallium nitride in which the degeneracy between different spin valence bands is lifted.

[1] T. Taliercio, P. Lefebvre, M. Gallart, and A. Morel, J. Phys.: Condens. Matter **13**, 7027 (2001).
[2] B. Beschoten, E. Johnston-Halperin, D. K. Young, M. Poggio, J. E. Grimaldi, S. Keller, S. P. DenBaars, U. K. Mishra, E. L. Hu, and D. D. Awschalom, Phys. Rev. B **63**, 121202(R) (2001).
[3] T. Kuroda, T. Yabushita, T. Kosuge, A. Tackeuchi, K. Taniguchi, T. Chinone, and N. Horio, Appl. Phys. Lett. **85**, 3116 (2004).
[4] H. Otake, T. Kuroda, T. Fujita, T. Ushiyama, A. Tackeuchi, T. Chinone, J.-H. Liang, and M. Kajikawa, Appl. Phys. Lett. **89**, 182110 (2006).
[5] A. Takeuchi, H. Otake, Y. Ogawa, T. Ushiyama, T. Fujita, F. Takano, and H. Akinaga, Appl. Phys. Lett. **88**, 162114 (2006).
[6] T. Ishiguro, Y. Toda, and S. Adachi, Appl. Phys. Lett. **90**, 011904 (2007).
[7] B. Beaumont, Ph. Vennéguès, and P. Gibart, Phys. Status Solidi B **227**, 43 (2001).
[8] Bernard Gil, Olivier Briot, and Roger-Louis Aulombard, Phys. Rev. B **52**, R17028 (1995).
[9] M. Joffre, D. Hulin, A. Migus, A. Antonetti, C. Benoit à la Guillaume, N. Peyghambarian, M. Lindberg, and S. W. Koch, Opt. Lett. **13**, 276 (1988).
[10] A. J. Fischer, W. Shan, G. H. Park, J. J. Song, D. S. Kim, D. S. Yee, R. Horning, and B. Goldenberg, Phys. Rev. B **56**, 1077 (1997).
[11] S. Pau, J. Kuhl, F. Scholz, V. Haerle, M. A. Khan, and C. J. Sun, Phys. Rev. B **56**, R12718 (1997).
[12] R. Zimmermann, A. Euteneuer, J. Möbius, D. Weber, M. R. Hofmann, W. W. Rühle, E. O. Göbel, B. K. Meyer, H. Amano, and I. Akasaki, Phys. Rev. B **56**, R12722 (1997).
[13] S. Pau, J. Kuhl, F. Scholz, V. Haerle, M. A. Khan, and C. J. Sun, Appl. Phys. Lett. **72**, 557 (1998).
[14] T. Aoki, G. Mohs, M. Kuwata-Gonokami, and A. A. Yamaguchi, Phys. Rev. Lett. **82**, 3108 (1999).
[15] H. Haag, B. Hönerlage, O. Briot and R. L. Aulombard, Phys. Rev. B **60**, 11624 (1999); H. Haag, P. Gilliot, R. Lévy, B. Hönerlage, O. Briot, S. Ruffenach-Clur, and R. L. Aulombard, Appl. Phys. Lett. **74**, 1436 (1999).
[16] M. Suzuki, T. Uenoyama, and A. Yanase, Phys. Rev. B **52**, 8132 (1995).
[17] K. Kyhm, R. A. Taylor, J. F. Ryan, T. Aoki, M. Kuwata-Gonokami, B. Beaumont, and P. Gibart, Phys. Rev. B **65**, 193102 (2002).
[18] G. L. Bir, A. G. Aronov, and G. E. Pikus, Zh. Eksp. Teor. Fiz. **69**, 1382 (1975) [Sov. Phys. JETP **42**, 705 (1976)]
[19] R. J. Elliot, Phys. Rev. **96**, 266 (1954).
[20] Y. Yafet, Solid State Phys. **14**, 1 (1963).
[21] Z. G. Yu, S. Krishnamurthy, M. vanSchilfgaarde and N. Newman, Phys. Rev. B **71**, 245312 (2005).
[22] M. I. D'yakonov and V. I. Perel', Zh. Eksp. Teor. Fiz. **65**, 362 (1973).
[23] D. Jena, Phys. Rev. B **70**, 245203 (2004).
[24] P. D. Brown, J. Cryst. Growth **210**, 143 (2000).
[25] M. Oestreich, S. Hallstein, A. P. Heberle, K. H. Schmidt, K. Eberl, E. Bauser, and W. W. Rühle, Phys. Rev. B **53**, 7911 (1996).
[26] D. J. Hilton and C. L. Tang, Phys. Rev. Lett. **89**, 146601 (2002).
[27] T. Uenoyama and L. J. Sham, Phys. Rev. Lett. **64**, 3070 (1990).
[28] R. Ferreira and G. Bastard, Phys. Rev. B **43**, 9687 (1991).
[29] S. Bar-Ad and I. Bar-Joseph, Phys. Rev. Lett. **68**, 349 (1992).
[30] R. Akimoto, K. Ando, F. Sasaki, S. Kobayashi, and T. Tani, Phys. Rev. B **56**, 9726 (1997).
[31] S. Adachi, T. Miyashita, S. Takeyama, Y. Takagi, and A. Tackeuchi, J. Lumin. **72**, 307 (1997).
[32] H. Rahimpour Soleimani, S. Cronenberger, M. Gallart, P. Gilliot, J. Cibert, O. Crégut, B. Hönerlage, and J.-P. Likforman, Appl. Phys. Lett. **87**, 192104 (2005).
[33] B. Baylac, X. Marie, T. Amand, M. Brousseau, J. Barrau, and Y. Shekun, Surf. Sci. **326**, 161 (1995).
[34] I. Brener, W. H. Knox, K. W. Goossen, and J. E. Cunningham, Phys. Rev. Lett. **70**, 319 (1993).
[35] T. Ostatnický, O. Crégut, M. Gallart, P. Gilliot, B. Hönerlage, and J.-P. Likforman, Phys. Rev. B **75**, 165311 (2007).